Evaluation and Prediction of the Effects of Melt-Processing Conditions on the Degree of Mixing in Alumina/Poly(ethylene terephthalate) Nanocomposites

Dongsik Kim, Jun S. Lee, Carol F. Barry, Joey L. Mead

Department of Plastics Engineering, University of Massachusetts at Lowell, One University Avenue, Lowell, Massachusetts 01854

Received 7 January 2008; accepted 6 March 2008
DOI 10.1002/app.28394
Published online 20 May 2008 in Wiley InterScience (www.interscience.wiley.com).

ABSTRACT: Alumina/poly(ethylene terephthalate) nanocomposites were prepared by melt compounding with a twin-screw extruder. The melt temperature, screw rotation speed, and feed rate were selected as important processing parameters, and their effects on the degree of mixing were studied with full-factorial, two-level experimental design. To quantitatively assess the effects of the processing parameters, the degree of mixing of the nanocomposites was evaluated by the skewness of the quadrat method based on the number of particles in transmission electron microscopy images. The screw speed was found to be the most important processing parameter controlling the degree of mixing under the conditions in this investigation. The specific energy input (SEI), related to the shear intensity, was found to correlate closely to the degree of mixing. The degree of mixing improved with increased SEI up to a limiting value, termed the critical SEI, indicating that there may be a critical value required for the optimum dispersion of a given system. A modeling approach was proposed to determine the critical SEI needed for complete mixing. Initial results showed that the critical SEI predicted by this model was within a factor of 3.5 of that obtained experimentally, demonstrating the utility of this approach for the dispersion of nanofillers. © 2008 Wiley Periodicals, Inc. J Appl Polym Sci 109: 2924–2934, 2008

Key words: compounding: extrusion; mixing; nanocomposites; simulations

INTRODUCTION

The class of materials known as nanocomposites has received increased interest since the initial development of clay/polyamide 6 (PA6) nanocomposites by the Toyota research group in the early 1990s.[1–3] Because of the large available surface area of nanoscopic particles, nanocomposites based on a relatively small amount of a properly dispersed nanofiller can provide substantial improvements in the heat distortion temperature,[4,5] strength and modulus,[4,6] flame resistance,[7–9] abrasion resistance,[10,11] and barrier properties,[4,12] even in comparison with conventional composites.

Nanoclays are the most extensively studied type of filler for polymeric nanocomposites. To improve the ease of dispersion, the interlayer cations present in these clays, such as Na^+ or Ca^{2+}, are generally ion-exchanged with organic cations, such as alkyl ammonium cations, whereas nonpolar organic polymers, such as polyolefins, are combined with polar additives, such as maleated polyolefins,[13] to improve dispersion. Until recently, most research has focused on the proper compatibilization of either the clay[12,14,15] or the polymer matrix.[16–18] The research and development of commercially viable manufacturing methods have been somewhat neglected.

In much of the initial work, nanocomposites were prepared by the *in situ* polymerization of a monomer/clay mixture. Although several attempts[5,19] to develop new classes of catalysts for *in situ* polymerization have successfully produced nanocomposites having superior properties compared to those prepared by conventional melt compounding, both the cost and complexity of such processes have limited their utilization; additionally, it has been reported that *in situ* polymerization may not always be sufficient to disperse all clay aggregates homogeneously in a polymeric matrix.[20] Melt processing can supply more energy to the aggregates to break them apart; it is also preferred as a standard industrial compounding technique, is environmentally benign because of the absence of a solvent and the lack of byproducts, and is also economically viable. Hence, more research has been directed toward investigating melt-compounding methods[21,22] and studying

Correspondence to: Dongsik Kim (nicedskim@gmail.com).
Contract grant sponsor: National Science Foundation; contract grant number: NSF-0425826.
Contract grant sponsor: William Hogan (past chancellor, University of Massachusetts, Lowell).
Contract grant sponsor: Commonwealth of Massachusetts through the John Adams Innovation Fund.

TABLE I
Summary of Previous Results for the Effect of the Processing Parameters[48]

Authors	Nanocomposite system	Results
Cho et al.[22]	Clay/PA6	Single-screw extrusion was far less effective in improving mechanical properties than twin-screw extrusion
Dennis et al.[33]	Clay/PA6	Extrusion must be optimized with respect to both the shear intensity and residence time simultaneously
Anderson[37]	Clay/PP	The most important factor for a twin-screw extruder is the feed location; the best results are obtained when all materials are fed together
Dolgovskij et al.[38]	Clay/PP-*g*-MA	Five different types of mixers were tested; a vertical, corotating twin-screw microcompounder gave the best result
Fasulo et al.[39]	Clay/TPO	A balance of processing parameters in twin-screw extrusion is required for the best results. Taken individually, a low temperature, a low feed rate, and a high screw speed were better for dispersion
Lertwimolnun and Vergnes[60]	Clay/PP	Processing parameters in batch mixing left the state of intercalation unaffected, although increasing the shear stress and mixing time and decreasing the temperature improved clay dispersion
Kim et al.[45]	Alumina/PET	A fill factor of about 0.70 was found to be optimal in batch mixing

PP-g-MA, maleic anhydride grafted PP; TPO, thermoplastic olefin.

systems such as polyamide (PA6),[6,23] polypropylene (PP),[24–29] polyesters,[30,31] and polycarbonate.[32]

The preparation of nanocomposites by melt processing means the use of compounding techniques such as batch mixing or extrusion. Within a heated mixing chamber, the polymer is melted at a high temperature and mechanically mixed with nanofillers to produce the nanocomposite. In these processes, polymer molecules gain increased mobility through the input of thermal energy, and the nanofillers are mechanically dispersed and mixed under the influence of shear forces. In this case, it is very important that the process parameters be understood and controlled. For example, a high temperature may help to improve the mobility of the polymer but will reduce the viscosity, resulting in less mechanical force being applied to the nanofillers and thus making it more difficult to break up filler agglomerates. Long residence times may improve mixing but may also enhance degradation and increase the cost of the process. The effective size of the filler particles in the composite is determined by the processing conditions as well as the compatibility with the matrix. Furthermore, the property enhancements depend primarily on the size, distribution, and orientation (in the case of high aspect ratios) of these particles. Maximizing the compatibility between the matrix and fillers is extremely important, but optimization of the processing and operational conditions of the compounding system is also very important, and the processing conditions must also be controlled to maximize property enhancements. Despite the importance of processing parameters on the final nanocomposite properties, only a few reports have considered their effects; the notable results are summarized in Table I.

Researchers have primarily concentrated on describing how the physical and mechanical properties are affected by the processing conditions, but they have given very few, if any, details regarding the quality of mixing in these systems. Because the preparation methods, as well as the materials in the composites, can affect the results, it is difficult to compare observations from different sources. Therefore, no summary of optimal processing conditions exists in the literature. To universally use and compare these data, a means of quantitatively evaluating the quality of nanocomposites is required. Properties can then be analyzed versus this quality factor. The degree of mixing in the resultant composites is a candidate for quality evaluation in nanocomposites, although there are difficulties in performing direct quantitative measurements of the degree of mixing because of the small size of the fillers.

Only a few researchers have attempted to evaluate nanocomposites in terms of the degree of mixing as measured by transmission electron microscopy (TEM)[23,33–36] or X-ray diffraction.[37,38] Relatively little can be found in the literature on the relationship between the degree of mixing and processing parameters and properties with the objective of optimizing the degree of mixing in terms of such parameters. Only two articles of which we are aware discuss the effects of the processing parameters in detail. Dennis et al.[33] measured the quality of mixing through TEM particle density but focused on the effects of the extruder type and screw configuration, rather than the processing conditions. Fasulo et al.[39] studied the effects of processing conditions, such as the temperature, feed rate, and screw speed, on mixing with twin-screw extrusion by experimental design. Although they evaluated the overall effects of the processing conditions, the specimens were ranked qualitatively by visual appearance, not quantitatively by more objective means.

A number of approaches have been developed to model the mixing of particulates into polymers. The

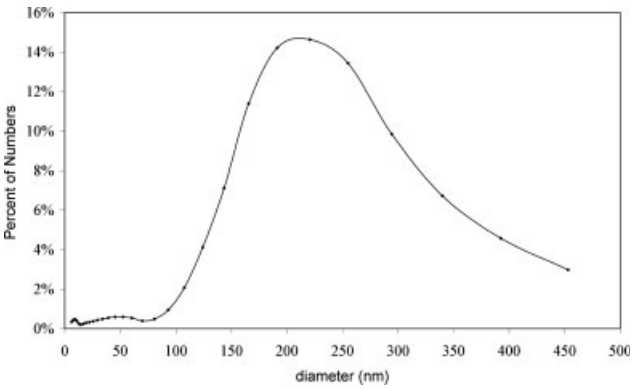

Figure 1 Size distribution of the alumina nanoparticles.

modeling of dispersive mixing in internal mixers based on the rupture theory for carbon black in rubber is well established.[40,41] Manas-Zloczower et al.[40,41] adapted Rumpf's equation[42] for the calculation of the cohesive force between aggregates and correlated the degree of dispersion with the ratio of the calculated hydrodynamic separating force and the cohesive force. Other methods to determine the cohesive force, such as those based on fracture mechanics,[43] have also been used. Rumpf's equation was found by Lee et al.[44] to be suitable for smaller particles, and this makes it attractive for applications with nanoparticles. Although these models simulate the mixing of internal mixers, models for mixing in twin-screw extruders are still rather limited because of the complexity of the twin-screw extrusion process. Furthermore, the degree of dispersion was evaluated by the measurement of the percentage of carbon black below 9 μm, which is not sufficient for nanocomposites.

The purpose of this study was to assess the effects of processing conditions on the degree of mixing with quantitative measurement of the quality of mixing in the nanocomposites and to use modeling to explain these effects. The results of this study should be broadly applicable to a range of nanocomposites and provide manufacturers the tools to optimize the processing conditions. This article reports results from twin-screw extrusion compounding, guided by experimental design to most efficiently determine the effects of the processing conditions on the degree of mixing of nanofillers in poly(ethylene terephthalate) (PET). In this study, spherical alumina nanoparticles were used as the nanofiller, eliminating issues related to orientation effects. As a quantitative index of the degree of mixing for nanocomposites, the quadrat method was applied to the nanocomposites, and the skewness (β) was calculated; the details and validity of β as an indicator of degree of mixing have been reported elsewhere.[45,46] The degree of mixing was correlated to a simplified model of the mixing process for a twin-screw extruder.

EXPERIMENTAL

Materials

Alumina (Al_2O_3) nanoparticles (average diameter = 48 nm) from Nanophase were used as received. PET pellets (Crystar PET from Dupont, Wilmington, DE; 0.55% DEG, intrinsic viscosity = 0.95 dL/g) were used after drying for 4 h in an oven at 120°C. The size distribution of the alumina nanoparticles was analyzed with a TSI model 3091 fast mobility particle sizer spectrometer. Although the primary particle size was reported to be 48 nm on average, the particles existed mostly as agglomerates, whose size ranged from 100 to 300 nm, as shown in Figure 1. No more than approximately 9% of particles had effective diameters of less than 100 nm.

Melt processing and parameters

PET and alumina nanoparticles were compounded with a corotating, intermeshing twin-screw extruder (ZSE 27 HP, Leistritz, Somerville, NJ; length/diameter = 40, diameter = 27 mm) under nitrogen. Three processing parameters (the melt temperature, extruder screw rotation speed, and feed rate) affecting the distribution and dispersion in compounding were selected, and the effect of each parameter was evaluated with two-level, full-factorial experimental design. The selected levels of each parameter are shown in Table II. The 10 temperature zones in the barrel were held constant at a single temperature during extrusion. Samples were collected after being quenched with cold water upon exiting the die. Although the feed location, filler amount, and screw configuration can affect the degree of mixing, they were fixed in this experiment. The mixture for the experiment was prepared with a mechanical premix of polymer pellets with the filler powder and was fed into the first section of the barrel, with the filler amount fixed at 2 wt %. To confirm the exact content of nanoalumina in each composite, samples were placed in a furnace at 800°C for 60 min, and the amount of residual ash was measured. Within experimental error, each sample contained the same amount

TABLE II
Matrix for the Experimental Design

Trial number	Temperature (°C)	Screw speed (rpm)	Feed rate (kg/h)
T-1	260	100	1
T-2	260	100	2
T-3	260	200	1
T-4	260	200	2
T-5	280	100	1
T-6	280	100	2
T-7	280	200	1
T-8	280	200	2

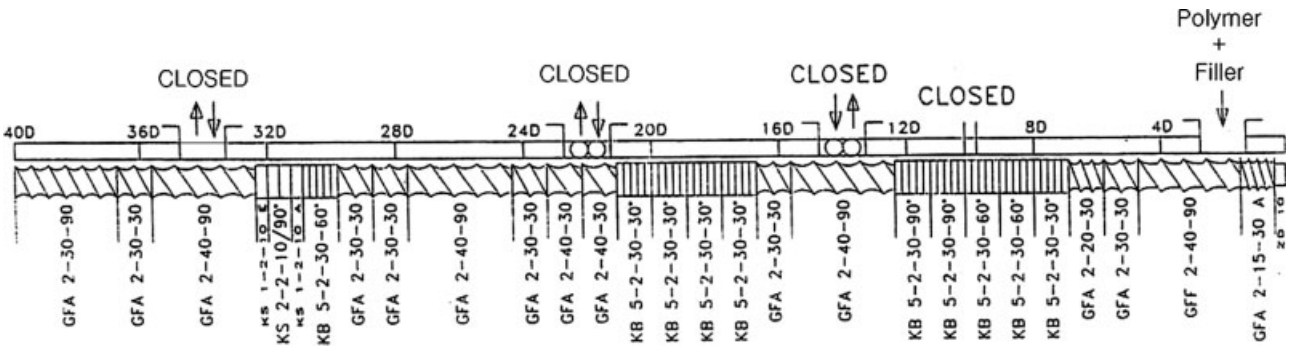

Figure 2 Screw configuration for the nanocomposite preparation.

of alumina (1.97 wt %). Although optimization of the screw configuration would be needed to balance the shearing and residence time distribution,[33] for simplicity only the fixed screw configuration shown in Figure 2 was used in this study, including three mixing zones to enhance mixing.

After this design of the experiment, three conditions for the best, medium, and worst mixing were repeated to determine the reproducibility (mixes T-1, T-4, and T-6, which are called T-A, T-B, and T-C, respectively). For these three conditions, nanocomposites with 5 wt % alumina were also prepared to evaluate the model with respect to different total agglomerate strengths [mixes T-1(5), T-4(5), and T-6(5)].

Characterization

Microscopy

TEM was used for analyzing the degree of mixing in the composites. Specimens for TEM analysis were taken from the extrudates randomly; the parts for sampling were separated by at least 3 min of extrusion time. Ultrathin sections from four different locations of each sample were cut with a diamond knife with a microtome and collected on 200-mesh copper TEM grids. The thin sections were examined by TEM with a Philips EM-400 with an accelerating voltage of 120 kV. The magnification was selected to be 22,000× to ensure that particles were distinguished and that the pictures included a sufficient number of aggregates and particles for statistical validity. Ten TEM images per trial were used for analysis.

Degree of mixing determined by the β–quadrat method[47]

β, derived from the quadrat method, was used to quantify the degree of mixing. Briefly, a TEM image is divided into small cells of equal size, called quadrats, and the number of particles in each quadrat is counted. Agglomerates are counted as single particles that belong to the cell in which their centers of gravity are located. Through the counting of the occurrence of the cells with equal numbers of particles and plotting of the frequency graph, the degree of asymmetry can be measured by β of the distribution, an index defined as follows:

$$\beta = \frac{q}{(q-1)(q-2)} \sum_{i=1}^{q} \left[\left(N_{qi} - N_q^{\text{mean}} \right) \Big/ \sigma \right]^3 \qquad (1)$$

where q is the total number of quadrats studied, N_{qi} is the number of particles in the ith quadrat, N_q^{mean} is the mean number of particles per quadrat, and σ is the standard deviation of the N_q distribution, which is the distribution of the number of particles in the guadrats. Because a composite with well-dispersed and uniformly distributed particles would be expected to have approximately the same number of particles in most of the quadrats, the plot of the number of particles per quadrat for this composite should have a bell-shaped distribution and a minimum degree of asymmetry (binomial or Poisson model). In contrast, a composite with chiefly aggregates would be expected to have some empty quadrats, some quadrats including a few particles, and some quadrats having many particles. The plot for this composite would then have an asymmetric shape and a high degree of asymmetry (negative binomial model). As a rule of thumb, smaller values of β mean less aggregation and better uniformity of the distribution. Additional details of this method have been described previously.[48]

In this study, a grid of 720 square cells was put on the TEM images, and N_{qi} was counted. Each cell had an area of 20,900 nm^2, which was sufficiently large versus the projected area of an individual particle 48 nm in diameter (1809 nm^2).

RESULTS AND DISCUSSION

Eight specimens of alumina/PET nanocomposites of identical composition were prepared in a twin-screw extruder with different processing parameters. Figure 3 shows representative images for each trial. The

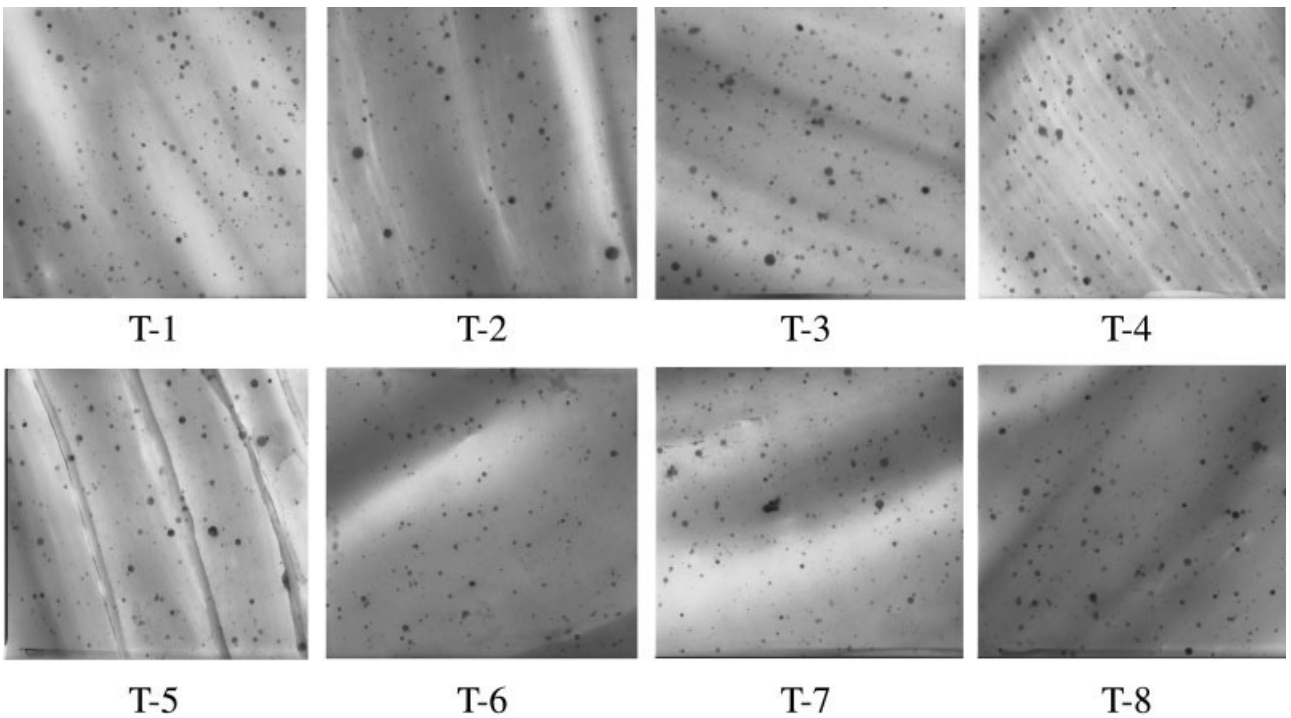

Figure 3 TEM images of alumina/PET nanocomposites (×22,000 magnification; each picture represents 3.8 μm × 3.5 μm).

approximate average sizes of the filler particles in the composites, estimated with TEM imaging, were much smaller than the agglomerate sizes before mixing (200 nm), as shown in Figure 1. Although some aggregates existed in composites prepared by a batch mixer under comparable processing conditions,[45] almost no aggregates greater than 100 nm in diameter were observed in these experiments. This work demonstrates that twin-screw extrusion is more effective than batch mixing in breaking up agglomerates and preparing well-mixed nanocomposites under the studied conditions.

Qualitatively, it is hard to differentiate and rank the TEM images of the composites in Figure 3, as they all appear similar. Quantification is required to analyze the effects of the various processing conditions. As the usefulness of the quantitative characterization method for nanocomposites has already been demonstrated,[45,46] these samples were therefore compared by the calculation of β via the quadrat method.

Effect of the process parameters on the degree of mixing by the β–quadrat method

The quadrat method has been used in the field of ecology, for instance, to analyze the distribution of nests of ant lions in a sandbox and has also been applied to the dispersion of small particles in composites.[49] Based on N_{qi}, the degree of asymmetry of

TABLE III
β Analysis for the Alumina/PET Nanocomposites

Trial number	Number of particles per cell	β	Rank for the degree of mixing
T-1	0.51 ± 0.03	3.7 ± 0.4	5
T-2	0.46 ± 0.03	4.8 ± 0.5	7
T-3	0.52 ± 0.02	3.6 ± 0.4	3
T-4	0.53 ± 0.02	3.3 ± 0.3	1
T-5	0.48 ± 0.03	4.3 ± 0.3	6
T-6	0.43 ± 0.02	5.3 ± 0.3	8
T-7	0.51 ± 0.03	3.6 ± 0.4	4
T-8	0.53 ± 0.04	3.4 ± 0.4	2
T-A	0.52 ± 0.02	3.6 ± 0.3	Repeat of T-1
T-B	0.53 ± 0.03	3.3 ± 0.5	Repeat of T-4
T-C	0.44 ± 0.02	5.1 ± 0.7	Repeat of T-6

TABLE IV
Summary of the Analysis from the Designed Experiments

Parameter	*F* ratio	Level	Mean
Temperature	10.4	260	3.86
		280	4.14
Screw speed	152.7	100	4.53
		200	3.47
Feed rate	21.4	1	3.80
		2	4.20
Temperature × speed	7.2	Critical *F* ratio	
Temperature × feed	60.0	F_{crit} = 2.15 at 95% confidence	
Speed × feed	0.0	F_{crit} = 2.92 at 99% confidence	
Temperature × speed × feed	0.0		

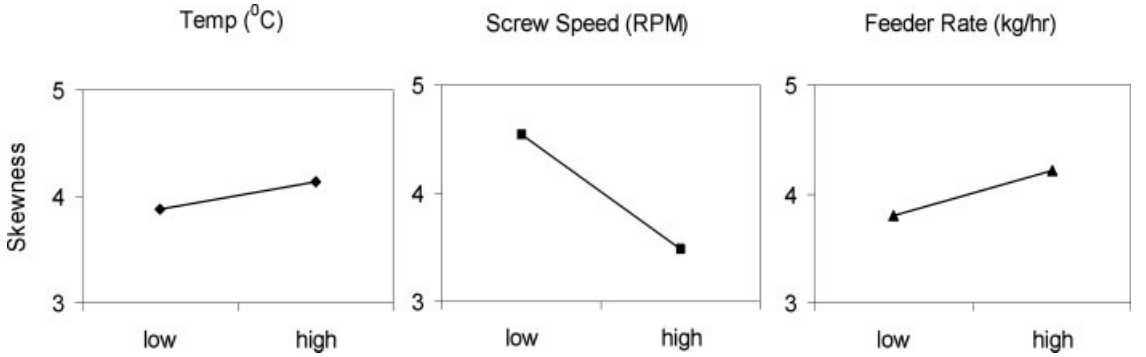

Figure 4 Graphs of the degree of mixing versus the processing parameters.

the frequency distribution in the quadrats was calculated with β for each sample and is summarized in Table III. These values are higher than those reported for grains in metal alloys, which have a range of 0.32–1.04[49] with 10–20 vol % of the second phase. This greater asymmetry observed in the nanocomposites was caused not by aggregation but rather by the fact that the samples had many empty quadrats as a result of the low filler content. To check the reproducibility of this experiment, three selected trials were repeated (T-A, T-B, and T-C were repeated for T-1, T-4, and T-6, respectively), and the values of β were consistent from run to run, as shown in Table III.

The F ratio of the analysis of variance[50] is 27.37 for this processing parameter study, higher than the critical F ratio (F_{crit}) of 2.92 at a 99% confidence level, and this makes the results statistically significant. Specific results from the analysis of the experimental design for individual and interacting parameters are summarized in Table IV. Except for the effects of the screw speed in combination with the feed rate and all three parameters combined, the other parameters and interactions are significant with respect to the degree of mixing, with the screw speed showing the most dominant effect. Figure 4 shows the trends for each parameter. The decrease in the degree of mixing can be explained by the change in the viscosity of the polymer. At lower temperatures, a higher viscosity helps to break up agglomerates via more shear stress, resulting in better mixing at lower temperatures. Similarly, a higher screw speed means higher shear rates applied to the agglomerates. These results indicate that the higher screw speeds result in better mixing despite the shorter residence time, giving nanocomposites with better distribution and dispersion. The feed rate is much more complicated because it may produce opposing factors of increasing shear rate and decreasing residence time (or vice versa). Consequently, the degree of mixing improves only with a higher screw speed and a lower feed rate, with the melt temperature appearing to have little effect under the studied conditions. Because some parameters produce greater effects in combination than in isolation, such as the melt temperature and feed rate, the prediction of optimized processing conditions is still very complicated. Further investigation of each parameter and the effect of the residence time and residence time distribution in terms of the degree of fill would be of interest for future work.

To understand the fundamental basis of the effects of the process parameters, we chose to evaluate the specific energy input (SEI) to the mix from the pro-

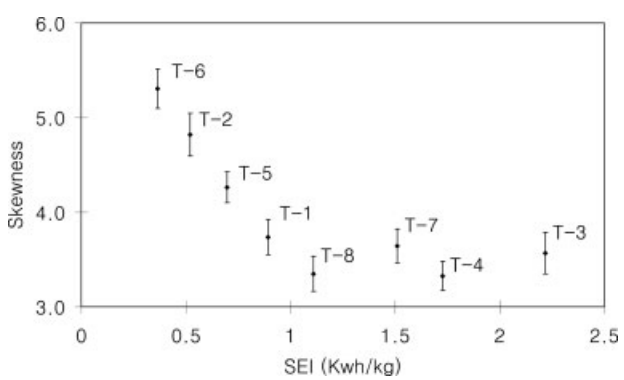

Figure 5 Graph of the degree of mixing versus SEI.

TABLE V
Summary of the Input Values Used in the Simulation for the Extruder Performance for Mix T-1

	Description	Value
Extruder	Screw diameter	27.0 Mm
	Revolution	1.7 rotation/s
Transport elements	Channel height	4.4 mm
	Channel width	5.5 mm
	Helix angle	0.1 rad
	Pitch	8.3 mm
	Flight width	1.7 mm
	Number of flights	2.0 each
	Output	213.7 mm^3/s
Clearance	Clearance	0.1 mm
	Relative width of flight	0.3

TABLE VI
Summary of the Calculated Values for the Extruder Performance for Mix T-1

	Description	Value
Extruder	Barrel velocity	141.4 mm/s
Transport elements	Drag flow	1684.2 mm^3/s
	Actual width	2.1 Mm
	Relative flight width	0.3
	Pressure flow	−1470.6 mm^3/s
	Pressure gradient	5870.9 Pa/mm
	Total force	311.3 N
	Total length	750.6 Mm
	Torque	4.2 Nm
Clearance	Leakage flow	39.9 mm^3/s
	Force	628.5 N
	Torque	8.5 Nm
Mixing elements	Corrected total output	487.1 mm^3/s
	Corrected actual width	9.0
	Leakage drag flow	1001.4 mm^3/s
	Relative flight length	0.3
	Recorrected output	1488.5 mm^3/s
	Drag flow	389.4 mm^3/s
	Pressure gradient	−22.3 Pa/mm
	Leakage flow	389.4 mm^3/s
	Total force	7566.7 N
	Total length	149.9 Mm
	Torque	102.2 Nm

cess parameters and correlate the results of the degree of mixing with SEI. SEI to the mix has been used to determine the amount of energy needed to create poly(vinyl alcohol) compositions that can be melt-extruded[51] and for the mixing of polymer–clay nanocomposites.[39] Although SEI to the mix was correlated to a better dispersion of the nanocomposites, no correlation between a required minimum or critical specific energy and optimum dispersion was determined. SEI can be used as a rough measure of the intensity of the shear processes:[52]

$$\text{Specific energy input} = \frac{E_{\max} \times {n_{\text{act}}}/{n_{\max}} \times T}{Q} \quad (2)$$

where $E_{\max}$ is the maximum available power for the extruder (kW); n_{act} and $n_{\max}$ are the actual and maximum screw rotation speeds (rpm), respectively; T is the torque measured during extrusion (%); and Q is the output rate (kg/h). A graph of the degree of mixing plotted against SEI shown in Figure 5 demonstrates a clear trend: The higher SEI is, the better the degree of mixing is up to a limiting value. Because mixing is likely to be strongly dependent on the shear intensity during processing, it is not surprising that the degree of mixing improves as SEI increases. Above SEI $\sim$ 1.1 kwh/kg, increasing SEI has no effect on the degree of mixing. These results support the concept that there is a critical SEI value required for a given system to obtain its maximum dispersion. These results would provide a method for determining the appropriate process parameters for a given polymer–filler system.

Simulation of the mixing process

To use the information for a different mixing process or different polymer–filler system, it is necessary to (1) determine SEI for a given set of processing conditions and (2) determine the required critical SEI value needed. Some approaches used to model the mixing process are described next.

To predict the mixing process, the Manas-Zloczower–Nir–Tadmor approach[40] has been widely adapted. This approach combines Rumph's model for the agglomerate strength with the hydrodynamic analysis for two touching rigid spheres in a simple shear flow. The fraction of broken agglomerates is dependent on a dimensionless fragmentation number (F_a):[53]

$$F_a = \frac{\mu\dot{\gamma}}{\sigma} \quad (3)$$

where σ is the tensile strength of the agglomerate and μ and $\dot{\gamma}$ are the viscosity and shear rate, respectively, in the process. This model was applied to a Banbury-type mixer and two-roll mills successfully.[41,54] There are, however, no reports of the application of this equation for a twin-screw extruder because of the complicated nature of the process. Other researchers have modeled corotating

TABLE VII
Summary of the Simulation Results

	Shear rate (1/s)		Degree of fill (%)		SEI (kwh/kg)	
Trial	Calcd	Approximation[58]	Calcd	Approximation[58]	Calcd	Actual
T-1	1400	1900	13	14	6.76	0.89
T-2	1400	1900	25	28	4.34	0.52
T-3	2800	3800	6	7	22.38	2.22
T-4	2800	3800	13	14	13.53	1.73
T-5	1400	1900	13	14	2.84	0.70
T-6	1400	1900	25	28	1.94	0.36
T-7	2800	3800	6	7	9.13	1.51
T-8	2800	3800	13	14	5.69	1.11

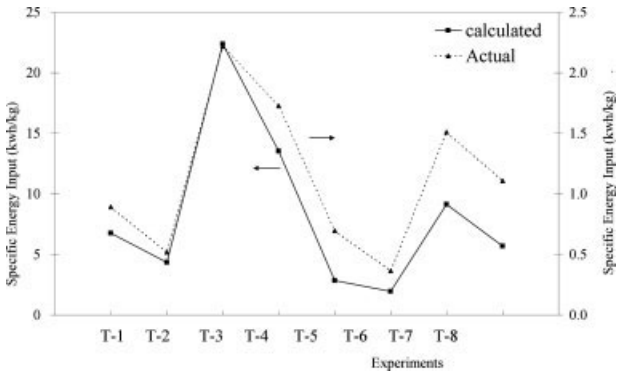

Figure 6 Comparison of the calculated and actual SEIs.

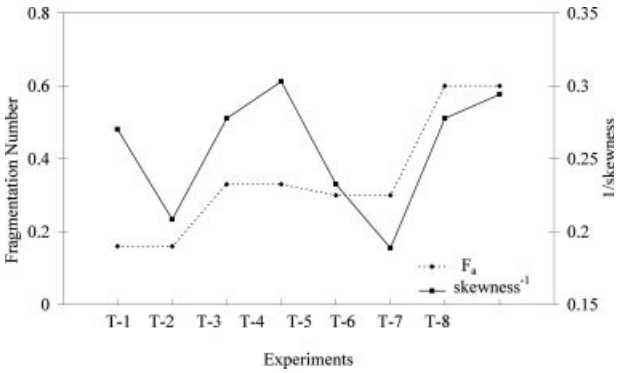

Figure 7 Comparison of the actual degree of mixing and calculation.

twin-screw extruders,[55,56] but they are very difficult to use because of the complications of treating the detailed complex geometry and the incompleteness of the model.

For this work, we attempted to predict the SEI values separately from the required critical specific energy. To predict the SEI values, we used Meijer and Elemans's approach[57] for a simplified calculation of the performance of a corotating twin-screw extruder without finite element analysis or numerical simulations. Their approach models a corotating twin-screw extruder as a single-screw extruder with the theories developed earlier. This approach uses general assumptions for modeling the extruder: (1) the model is isothermal and Newtonian; (2) there is no distinguished melting mechanism; (3) the screw is stationary, and the barrel is rotating; (4) curvatures can be neglected; (5) the screw channel is considered to have a rectangular cross-sectional shape, with an average height and width; and (6) different zones are considered together (e.g., separate mixing zones are treated as one long mixing zone for simplicity). Table V summarizes the input values from the measurements of the process and the characteristics of the extruder for representative mix T-1. Table VI shows the calculated values from the simulation. The calculated values for the shear rate and the degree of fill are in reasonably good accord with the values attained from the recommended rough approximations by Martin[58] (see Table VII). Several assumptions were not applicable to the real system, so the calculated SEI values were higher than the actual SEI values measured from the experiments; however, the trends and ratios of the calculated and actual values were consistent (see Fig. 6). If a correction factor, which is about 7 in this experiment, is applied, the calculations could simulate the real process. Table VII summarizes the calculations and comparisons of the shear rate, degree of fill, and SEI for every trial conducted in the experiments.

To use this approach for a wide array of materials, it is important to determine the required critical SEI for a given system. This should be related to the interaction strength between aggregates. To estimate this value, the tensile cohesive strength (σ) between the aggregates was calculated with Rumpf's equation:[42]

$$\sigma \approx \frac{H}{48rz_0^2}\frac{\phi}{1-\phi} \tag{4}$$

where H is the Hamaker constant ($H \approx 1.5 \times 10^{-19}$ J for aluminum oxide[59]), r is the radius of the primary particles, z_0 is the separation distance (typically 0.4

TABLE VIII
Calculation of the Critical SEI

	2 wt %	5 wt %
Tensile strength (Rumpf's equation; Pa)	1.3×10^6	
Radius of the primary particle (m)	2.2×10^{-8}	
Agglomerate volume (d = 500 nm; m^3)	6.5×10^{-20}	
Solid volume in agglomerate (assume FCC; m^3)	4.8×10^{-20}	
Number of particles in an agglomerate	1.2×10^3	
Total cross-sectional area of particles in an agglomerate (m^2)	1.7×10^{-12}	
Average distance between particles in perfect mixing (m)	1.8×10^{-7}	1.2×10^{-7}
Energy to break per agglomerate (J)	2.0×10^{-13}	1.3×10^{-13}
Number of breaks	20	
Number of agglomerates/kg of PET	1.2×10^{14}	2.9×10^{14}
Total energy/kg of PET (kwh/kg)	0.13	0.21
Critical SEI including ΔH_f and efficiency (kwh/kg)	0.32	0.50

FCC, face-centered cubic.

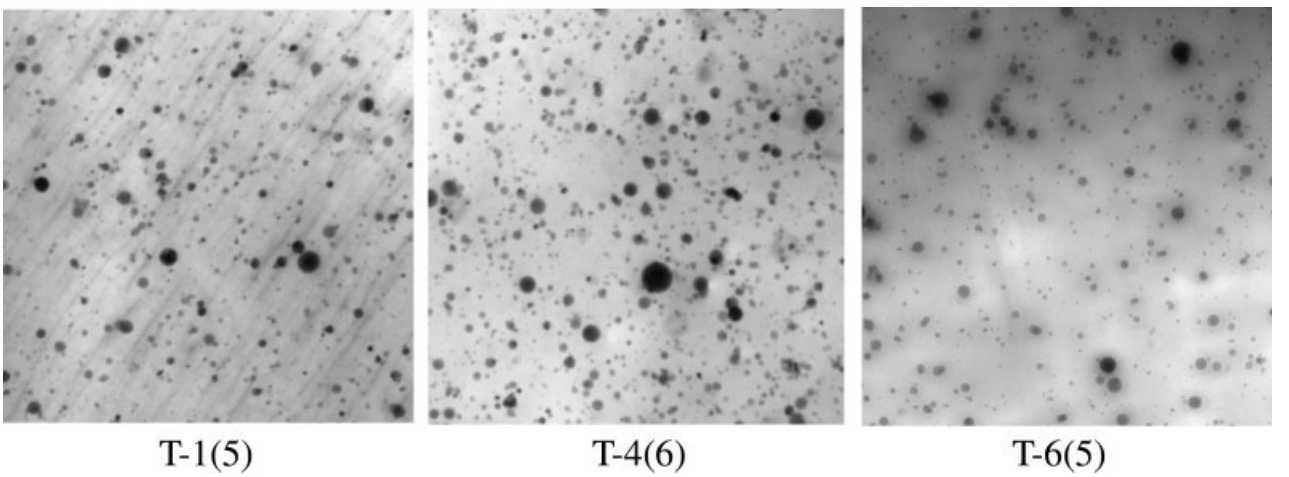

Figure 8 TEM images of 5 wt % alumina/PET nanocomposites (each picture represents 3.7 μm × 3.7 μm).

nm[40]), and ϕ is the volume fraction of solids. If the ideal conditions are assumed, which means spatially uniform and identical spheres bound to neighbors by van der Waals forces, σ for nanoalumina particles is calculated to be 1.3 MPa, which is the force for a single fracture of the agglomerate.

The results from the SEI calculation (Meijer) and the cohesive strength calculation were then input into the Manas-Zloczower–Nir–Tadmor model.[54] Figure 7 shows a comparison of the degree of mixing ($1/\beta$) and the calculation from the Manas-Zloczower–Nir–Tadmor model[54] for agglomerate dispersion in simple shear flow with the aforementioned calculation for the separation of two particles. The model can predict the trend reasonably well, although the values have a discrepancy because (1) real particles have a wide range of size distributions, (2) agglomerates were not completely dispersed into primary particles, (3) the viscosity was varied at points throughout the process, (4) the actual mixing process experienced a complex combination of shear and elongation deformations, and (5) the system is not an ideal case as assumed previously. Clearly, this model could be improved to better simulate this process, including the effect of the feed rate on the mixing coupled with the degree of fill.

To understand the significance of the critical SEI value for mixing, the total required energy to reach the ideal maximum mixing was calculated with Rumpf's equation for a composite system with a 2 wt % loading. If we assume that (1) the uniform spherical particles are randomly packed into an isotropic and homogeneous agglomerate, (2) the initial agglomerate is also uniform in diameter (500 nm), and (3) after 20 fragmentations, each agglomerate breaks into all primary particles, the required energy for this composite system can be calculated to be approximately 0.13 kwh/kg, as shown in Table VIII. If the efficiency of the extruder is 50% and the heat of fusion is included, the total required energy for perfect mixing can be calculated to be 0.32 kwh/kg. The experimentally determined critical SEI was 1.1 kwh/kg, a factor of 3.5 higher, but within reason because of the number of approximations used in the model.

This modeling approach was also applied to the 5 wt % alumina/PET nanocomposites, and the corrected critical SEI value was calculated to be 1.7 kwh/kg (Table VIII) with the correction factor of 3.5. Three selected trials, T-1(5), T-4(5), and T-6(5), were prepared with 5 wt % nanoalumina with the designated processing conditions, and the TEM pictures are presented in Figure 8. Table IX summarizes the

TABLE IX
Experimental Analysis for 5 wt % Alumina

Trial number	Number of particles per cell	β	SEI (kwh/kg)
T-1(5)	0.26 ± 0.01	13.0 ± 1.0	0.92 ± 0.18
T-4(5)	0.29 ± 0.01	9.6 ± 0.8	1.82 ± 0.16
T-6(5)	0.24 ± 0.01	15.5 ± 1.1	0.40 ± 0.19

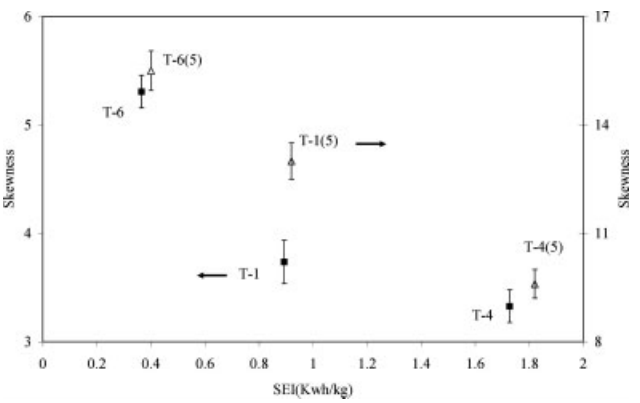

Figure 9 Comparisons of the effects of SEI on mixing for two different filler amounts.

analysis of β, normalizing the number of particles to the 2 wt % composites, as well as the actual SEI for each trial. As expected from the aforementioned calculation, a higher loading required more energy to disperse the particles, resulting in poorer mixing for the 5 wt % samples compared to the 2 wt % samples under the same processing conditions. With respect to a critical SEI value, the degree of mixing continuously improved with increasing SEI, as shown in Figure 9, because the estimated critical SEI was 1.7 kwh/kg, the highest SEI of the mixes prepared.

CONCLUSIONS

The effects of several processing parameters on the degree of mixing were investigated in a melt-compounded alumina nanoparticle/PET nanocomposite system. Three processing parameters in a twin-screw extrusion process were selected: the melt temperature, screw speed, and feed rate. The degree of mixing was quantified with β, as calculated by the quadrat method, which can measure the degree of mixing quantitatively. The overall effects of each parameter on the degree of mixing were evaluated through full-factorial, two-level experimental design. The screw speed was found to have the strongest effect on the degree of mixing; with better mixing observed at higher screw speeds. The feed rate also had a significant effect, with the lower feed rate giving better mixing. Lower melt temperatures also led to an improved degree of mixing. It was found that SEI to the mix was a good indicator of the degree of mixing. The degree of mixing improved with SEI increasing up to a limiting value, which was termed the critical SEI, and this indicated that there may be a critical value required for the optimum dispersion of a given system. This approach allows for variations in the process parameters, while still maintaining good dispersion, provided that a critical SEI value is maintained.

A modeling approach was proposed to allow for the determination of the critical SEI for a range of different polymer–filler systems. Initial results showed that the critical SEI predicted by this model was within a factor of 3.5 of that obtained experimentally, indicating the potential for this approach. This was further confirmed by the use of the model to predict the amount of energy required to disperse two different filler loadings. It was demonstrated experimentally that a 5 wt % filler loaded composite required a higher critical SEI and was harder to disperse than a 2 wt % filler loaded composite as predicted by the model.

As processing parameters can affect the degree of mixing for nanocomposites, proper selection and optimization of processing guided by modeling offer a significant advantage for the application of nanoscale fillers. This study demonstrates the potential to use the critical SEI value as a way of developing the optimum dispersion of nanoscale fillers in a twin-screw extrusion process.

The authors thank Albany International for donating materials. The authors especially thank Linda Schadler and Rahmi Ozisik of Rensselaer Polytechnic Institute, Gregory Toney of Albany International Co., and Daniel Schmidt of the University of Massachusetts at Lowell for their helpful discussions.

References

1. Okada, A.; Kawasumi, M.; Usuki, A.; Kojima, Y.; Kurauchi, T.; Kamigaito, O. MRS Symp Proc 1990, 171, 45.
2. Usuki, A.; Kawasumi, M.; Kojima, Y.; Okada, A.; Kurauchi, T.; Kamigaito, O. J Mater Res 1993, 8, 1174.
3. Kojima, Y.; Usuki, A.; Kawasumi, M.; Okada, A.; Kurauchi, T.; Kamigaito, O. J Polym Sci Part A: Polym Chem 1993, 31, 983.
4. Alexandre, M.; Dubois, P. Mater Sci Eng R 2000, 28, 1.
5. Ma, J.; Qi, Z.; Hu, Y. J Appl Polym Sci 2001, 82, 3611.
6. Liu, L.; Qi, Z.; Zhu, X. J Appl Polym Sci 1999, 71, 1133.
7. Gilman, J. W.; Kashiwagi, T. Int SAMPE Symp 1997, 42, 1078.
8. Gilman, J. W. Appl Clay Sci 1999, 15, 31.
9. Gilman, J. W.; Jackson, C. L.; Morgan, A. B.; Harris, R.; Marinas, E.; Giannelis, E.; Wuthenow, M.; Hilton, D.; Philips, S. H. Chem Mater 2000, 12, 1866.
10. Sawyer, W. G.; Freudenberg, K. D.; Bhimaraj, P.; Schadler, L. S. Wear 2003, 254, 573.
11. Bhimaraj, P.; Burris, D. L.; Action, J.; Sawyer, W. G.; Toney, C. G.; Siegel, R. W.; Schadler, L. S. Wear 2005, 258, 1437.
12. Hotta, S.; Paul, D. R. Polymer 2004, 45, 7639.
13. Kang, D.; Kim, D.; Yoon, S.-H.; Kim, D.; Barry, C. F.; Mead, J. L. Macromol Mater Eng 2007, 292, 329.
14. Doh, J. G.; Cho, I. Polym Bull 1998, 41, 511.
15. Fornes, T. D.; Yoon, P. J.; Hunter, D. L.; Keskkula, H.; Paul, D. R. Polymer 2002, 43, 5915.
16. Wang, K. H.; Choi, M. H.; Koo, C. M.; Choi, Y. S.; Chung, I. J. Polymer 2001, 42, 9819.
17. Chow, W. S.; Mohd, I. Z. A.; Karger-Kocsis, J.; Apostolov, A. A.; Ishiaku, U. S. Polymer 2003, 44, 7427.
18. Wang, Y.; Chen, F.-B.; Li, Y.-C.; Wu, K.-C. Compos B 2004, 35, 111.
19. Bergman, J.; Chen, H.; Giannelis, E.; Thomas, M.; Coates, G. Chem Commun 1999, 21, 2179.
20. Sun, T.; Garces, J. Adv Mater 2002, 14, 128.
21. Vaia, R. A.; Ishii, H.; Giannelis, E. P. Chem Mater 1993, 5, 1694.
22. Cho, J. W.; Paul, D. R. Polymer 2001, 42, 1083.
23. Fornes, T. D.; Yoon, P. J.; Keskkula, H.; Paul, D. R. Polymer 2001, 42, 9929.
24. Usuki, A.; Kato, M.; Okada, A.; Kurauchi, T. J Appl Polym Sci 1997, 63, 137.
25. Kawasumi, M.; Hasegawa, N.; Kato, M.; Usuki, A.; Okada, A. Macromolecules 1997, 30, 6333.
26. Hasegawa, N.; Kawasumi, M.; Kato, M.; Usuki, A.; Okada, A. J Appl Polym Sci 1998, 67, 87.
27. Nam, P. H.; Maiti, P.; Okamoto, M.; Kotaka, T.; Hasegawa, N.; Usuki, A. Polymer 2001, 42, 9633.
28. Liu, X.; Wu, Q. Polymer 2001, 42, 10013.
29. Kaempfer, D.; Thomann, R.; Mulhaupt, R. Polymer 2002, 43, 2909.
30. Davis, C. H.; Mathias, L. J.; Gilman, J. W.; Schiraldi, D. A.; Shields, J. R.; Trulove, P.; Sutto, T. E.; Delong, H. C. J Polym Sci Part B: Polym Phys 2002, 40, 2661.

31. Chisholm, B. J.; Moore, R. B.; Barber, G.; Khouri, F.; Hempstead, A.; Larsen, M.; Olson, E.; Kelley, J.; Balch, G.; Caraher, J. Macromolecules 2002, 35, 5508.
32. Huang, X.; Lewis, S.; Brittain, W. J.; Vaia, R. A. Macromolecules 2000, 33, 2000.
33. Dennis, H. R.; Hunter, D. L.; Chang, D.; Kim, S.; White, J. L.; Cho, J. W.; Paul, D. R. Polymer 2001, 42, 9513.
34. Manias, E.; Touny, A.; Wu, L.; Strawhecker, K.; Lu, B.; Chung, T. Chem Mater 2001, 13, 3516.
35. Eckel, D. F.; Balogh, M. P.; Fasulo, P. D.; Rodgers, W. R. J Appl Polym Sci 2004, 93, 1110.
36. Ratinac, K. R.; Gilbert, P. G.; Ye, L.; Jones, A. S.; Ringer, S. P. Polymer 2006, 47, 6337.
37. Anderson, P. G. Soc Plast Eng Annu Tech Conf 2002, 48.
38. Dolgovskij, M. K.; Fasulo, P. D.; Lortie, F.; Macosko, C. W.; Ottaviani, R. A.; Rodgers, W. R. Soc Plast Eng Annu Tech Conf 2003, 49, 2255.
39. Fasulo, P. D.; Rodgers, W. R.; Ottaviani, R. A.; Hunter, D. L. Polym Eng Sci 2004, 44, 1036.
40. Manas-Zloczower, I.; Nir, A.; Tadmor, Z. Rubber Chem Technol 1982, 55, 1250.
41. Manas-Zloczower, I.; Nir, A.; Tadmor, Z. Rubber Chem Technol 1984, 57, 583.
42. Rumpf, H. The Strength of Granules and Agglomerates; Wiley-Interscience: New York, 1962.
43. Kendall, K. Powder Metall 1988, 31, 28.
44. Lee, Y. J.; Feke, D. L.; Zloczower, I. M. Chem Eng Sci 1993, 48, 3363.
45. Kim, D.; Lee, J. S.; Barry, C. M. F.; Mead, J. L. Polym Eng Sci 2007, 47, 2049.
46. Kim, D.; Lee, J. S.; Barry, C. F.; Mead, J. L. Microsc Res Technol 2007, 70, 539.
47. Rogers, A. Statistical Analysis of Spatial Dispersion: The Quadrat Method; Pion: London, 1974.
48. Kim, D.; Lee, J. S.; Barry, C. F.; Mead, J. L. Mater Sci Technol 2006, 2, 333.
49. Karnezis, P. A.; Durrant, G.; Cantor, B. Mater Char 1998, 40, 97.
50. http://www2.chass.ncsu.edu/garson/pa765/anova.htm (accessed April, 2006).
51. Famili, A.; Nangeroni, J. F.; Marten, F. L. U.S. Pat. 5,362,778 (1994).
52. Todd, D. B. Plastics Compounding: Equipment and Processing; Hanser: Munich, 1998.
53. Ottino, J. M.; DeRoussel, P.; Hansen, S.; Khakhar, D. V. Adv Chem Eng 2000, 25, 105.
54. Manas-Zloczower, I.; Nir, A.; Tadmor, Z. Polym Comp 1985, 6, 222.
55. Rauwendaal, C. J. Polymer Extrusion; Hanser: Munich, 1986.
56. Jansen, L. P. B. M. Twin Screw Extrusion; Elsevier: Amsterdam, 1978.
57. Meijer, H. E. H.; Elemans, P. H. M. Polym Eng Sci 1988, 28, 275.
58. Martin, C. Plast M&A 2006.
59. Liu, J. C.; Jean, J. H.; Li, C. C. J Am Ceramic Soc 2006, 89, 882.
60. Lertwimolnun, W.; Vergnes, B. Polymer 2005, 46, 3462.